TECHNICAL UNIVERSITY OF LIBEREC

Faculty of Mechatronics and Interdisciplinary
Engineering Studies
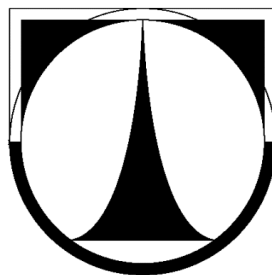
NOISE AND VIBRATION CONTROL USING PIEZOELECTRIC ELEMENTS SHUNTED BY A NEGATIVE CAPACITOR

REPORT OF THE PH.D. THESIS

2007   TOMÁŠ SLUKA

NOISE AND VIBRATION CONTROL USING PIEZOELECTRIC ELEMENTS SHUNTED BY A NEGATIVE CAPACITOR

TLUMENÍ HLUKU A VIBRACÍ POMOCÍ PIEZOELEKTRICKÉHO ELEMENTU A ELEKTRICKÉHO JEDNOBRANU SE ZÁPORNOU KAPACITOU

REPORT OF THE PH.D. THESIS

Doctoral candidate:	Tomáš Sluka
Study programme:	2612V Electrical Engineering and Computer Science
Specialization area:	3901V025 Science Engineering
Department:	Institute of Mechatronics and Computer Engineering
	Faculty of Mechatronics and Interdisciplinary
	Engineering Studies
	Technical University of Liberec
Supervisor:	Doc. Ing. Pavel Mokrý, PhD.

WORK EXTENT:

Number of pages:	178
Number of figures:	66
Number of tables:	10
Number of appendixes:	5

Annotation

A theoretical and experimental study of the vibration isolation and noise shielding systems is presented in this Thesis. The systems utilize the imbedded piezoelectric transducers whose an effective elastic response is controlled by a one-port shunt electrical network that behaves as a negative capacitor. This concept combines the advantages of the fast analog circuits and both a direct and an inverse piezoelectric effects to realize control systems with an ideal collocation of sensing and an actuation of controlled mechanical or acoustic quantity.

The vibration isolation system is realized by a piezoelectric stack actuator, which is shunted with a negative capacitor and placed between a source of vibrations and a passive mechanical structure. The elastic response of the actuator is controlled by the negative capacitor in order to suppress the vibration transmission, which occurs when the effective dynamic elastic stiffness of the actuator is manifested as extremely small or, in theory, zero.

The noise shielding system is realized by a cylindrically curved piezoelectric membrane, which is connected to the negative capacitor and fixed in an acoustic tube between a speaker and a silenced volume. The radial motion of the membrane in the sound field is controlled by the negative capacitor in order to reflect the majority of incident acoustic energy. This occurs when the membrane responds as an extremely hard acoustic element.

The described fundamental concepts suffer from high sensitivity of their efficiency to variations in the operating conditions. The proper function of the systems is crucially dependent on the accuracy of matching between capacitances of the piezoelectric transducer and the negative capacitor. Therefore, the main deal of the presented Thesis lies in the theoretical analysis and the consequent design of a mechanism which adapts the parameters of the system to the changes in operating conditions. The adaptation is achieved by an implementation of additional error sensors and control circuits that keep the proper adjustment of the analog negative capacitor.

The designed adaptive systems were realized and tested in experimental apparatuses and a positive effect of the implemented adaptation on the system efficiency is verified at a single harmonic component of frequency spectra.

Anotace

Disertační práce se věnuje teoretické a experimentální studii systémů pro potlačování přenosu vibrací a hluku. Systémy využívají zabudovaných piezoelektrických převodníků jejichž efektivní elastická odezva je řízena elektrickým dvojpólovým bočníkem, který se chová jako kondenzátor se zápornou kapacitou. Tato koncepce spojuje výhody rychlého analogového obvodu a jak přímého tak nepřímého piezoelektrického jevu k vytvoření řídicích systémů, které umožňují dokonalou kolokaci míst snímání a zasahování do řízené veličiny.

Systém pro potlačení přenosu vibrací je vytvořen pomocí piezoelektrického vrstvového aktuátoru, který je paralelně spojen s kondenzátorem se zápornou kapacitou a vložen mezi zdroj vibrací a pasivní mechanickou konstrukci. Elastická odezva aktuátoru je řízena tak, aby byl potlačen přenos vibrací ze zdroje na mechanickou konstrukci, což nastane, když se efektivní dynamická tuhost aktuátoru jeví jako mimořádně malá, teoreticky nulová.

Systém pro potlačování přenosu hluku je realizován pomocí zakřivené piezoelektrické membrány, která je připojena ke kondenzátoru se zápornou kapacitou a upevněna ve zvukové trubici mezi reproduktor a odhlučňovaný prostor. Radiální pohyb membrány ve zvukovém poli je řízen tak, aby většina dopadající zvukové energie byla odrážena. Toto nastane, pokud se membrána jeví jako akusticky mimořádně tuhý prvek.

Uvedená základní koncepce trpí vysokou citlivostí efektivity obou systémů na změny provozních podmínek. Správná funkce systémů je kriticky závislá na přesnosti shody velikosti a fáze kapacit piezoelektrického prvku a kondenzátoru se zápornou kapacitou. Z tohoto důvodu, stěžejní úkol předkládané disertační práce spočívá v teoretické analýze systémů a následném návrhu mechanismu přizpůsobování parametrů systému změnám v provozních podmínkách. Přizpůsobování je dosaženo doplněním systémů o snímače chybové veličiny a řídicí obvody, které udržují požadované nastavení analogového kondenzátoru se zápornou kapacitou.

Návrh adaptivních systémů byl realizován a testován v experimentální aparatuře, kde byl ověřen příznivý vliv navrženého přizpůsobování na jedné složce frekvenčního spektra.

Contents

INTRODUCTION

Continuously accelerating technical progress entails a number of disserviceable side-effects one of which is an increasing noisiness of the environment. Noise is currently perceived as an environmental pollutant due to its negative impact on human psyche, hearing, and living comfort. On that account, a noise reduction has become a highly important parameter regarded with the process of development mainly in civil engineering, automotive industry, and aerospace industry. This attitude has wide-ranging economic and also legislative consequences and means a new challenge for researchers and developers in broad variety of scientific fields with a strong accent on the interdisciplinary interaction. Another than the environment related demands for a high performance noise control emerge mainly from the need for an essential protection of human hearing or high precision devices in extreme acoustic conditions such as in pilot cockpits.

An effective noise reduction is often achieved via a vibration control of the mechanical structures that are sources of sound or interfaces in a sound propagation path. For that reason, progress in the noise control has always largely reflected current state of the vibration control technologies. The vibration control itself is important for the essential protection of mechanical structures and devices against damage or aging of their vibrating parts and consequently for the increase of their reliability, safety, and prolongation of useful life. Another purpose of the vibration control is found in providing essential or better conditions for operation of high precision devices.

Contemporary noise and vibration control techniques are based mostly on (i) properties of the passive elements such as massive walls and porous materials in case of noise control and springs, mass, and viscoelastic dampers in vibration control, or (ii) conventional active feedback and feedforward control principles. Each of these two concepts has its own advantages in specific contexts. Generally, the passive methods are rather inexpensive, do not require an external source of energy, but are bulky and weighty relatively to their efficiency. On the other hand, the methods based on conventional active control principles can achieve an excellent efficiency with a subtle device, but on the expense of high technical complexity, the higher costs, and the lower reliability.

There is necessarily a gap between the conventional passive and active noise

and vibration control methods which miss a set of devices effectively balancing advantages of both conventional approaches: a high efficiency, an undemanding technical performance, a minimal weight and size, a low cost, and a small or no need for an external power supply.

A promising new approach came with utilization of smart materials in a novel intelligent way based on simultaneous sensing and actuation performed by a single monolithic smart sample which is controlled by one-port shunt circuits. This technique is in literature commonly referred to as a *piezoelectric shunt damping* (PSD). Since this Thesis works up generalized principles of PSD methods for purposes in which in fact no intentional damping occurs, the term *piezoelectric shunt acoustic control* (PSAC) is suggested and further used in this text as the more general term covering also PSD methods as a subgroup.

The PSAC methods have been heralded as the dawn of a new era in the construction of automotive vehicles, airplanes, and other structures that have to meet ever more demanding performance requirements. This has largely not happened, at least not in the commercial arena. Therefore, despite potentials of the PSAC methods, yet most applications still remain confined to a pre-development stage in research laboratories and both fundamental studies and interdisciplinary engineering research need to be carried out in order to bridge the gap between academic and industrial environment. The presented Thesis intends to contribute to this effort.

1.1   Piezoelectric Shunt Acoustic Control

Various simple one-port active and passive electric circuits significantly influence the dynamic mechanical response of the piezoelectric elements which they are connected to. Such elements can be profitably utilized in the noise and vibration control systems as the parts with the desired effective mechanical or acoustical properties. The basic idea of PSAC is shown in Fig. 1.1 (a) for the vibration control and (b) for the noise control in a duct. This alternative approach to the noise and vibration control emerged from the works of Forward and Swigert [1, 2]. They used a single piezoelectric element imbedded to a vibrating structure as the electromechanical transducer mediating the interaction between the structure and the electrical shunt circuit (a passive resistor).

Further modifications of PSAC are based on the same principle, where the electromechanical interaction of mechanical structures or acoustic systems with various active or passive electrical shunt circuits is provided fundamentally by a single piezoelectric element. Various PSAC realizations differ in the form of the emplacement of piezoelectric elements, the electrical network of shunt circuits, and some other particular modifications.
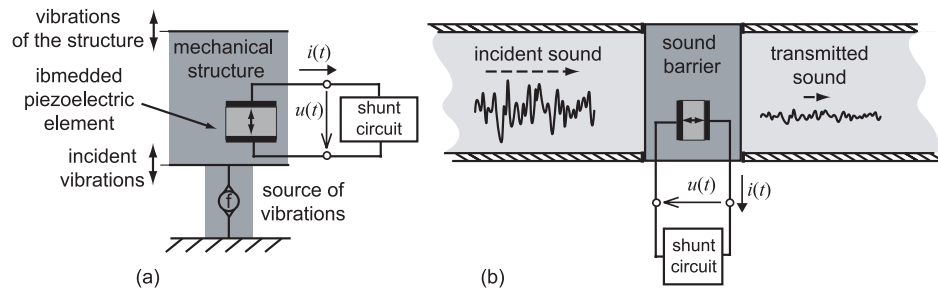
Figure 1.1: A fundamental concept of PSAC of (a) vibrations and (b) sound transmission. The piezoelectric element is imbedded into the mechanical or acoustical system, which is subjected to vibrations or acoustic pressure. Piezo-electric element mediates the interaction between the system and the one-port electric shunt circuit.

1.2 Shunt circuit topologies

Shunt circuits can be primarily categorized into passive and active and linear and nonlinear. Various approaches with resonant, resistive, capacitive, and switching shunts have been developed in the past as it is summarized in Fig. 1.2 (introduced by Niederberger [3]). The majority of the works published earlier in the field of PSAC has focussed on the resonant shunts for the vibration control and mainly on the vibration damping.

   This Thesis studies the subset of active linear shunt circuits (negative capacitors) and their utilization in vibration isolation and noise shielding systems.

Negative capacitors Recently, a generalized active PSAC method has been developed by Date et al. [4]. It was demonstrated that by connecting the piezoelectric element to a negative capacitor, it is possible to control the effective elastic stiffness of the piezoelectric element to extremely large extent actively, in theory to zero or infinity, in a broad frequency range. This method allows to realize noise shielding and vibration isolation systems.

The method of noise shielding by PSAC with a negative capacitor is based on the principle that the sound propagation through the curved membrane in air is controlled by the ratio of specific acoustic impedances of air and membrane. Since the specific acoustic impedance of the curved membrane fixed in a rigid frame is proportional to its elastic stiffness, an extremely stiff membrane (compared to air) works as an interface with high sound transmission loss. In this arrangement, the majority of acoustic energy is reflected from the membrane and only a negligible amount of energy is transmitted or absorbed.
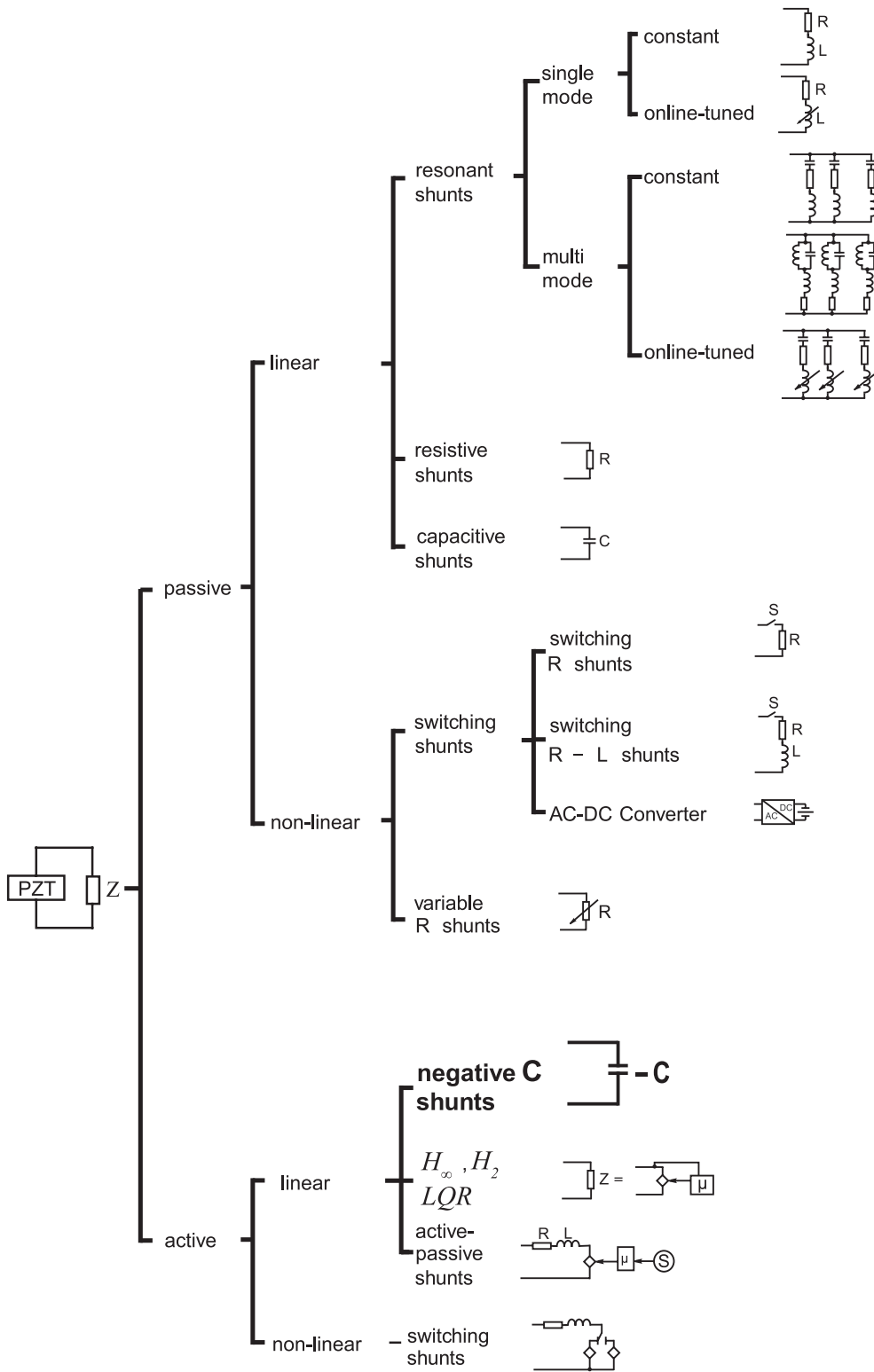
Figure 1.2: Categorization of shunt circuits (adopted from [3]).

The vibration isolation is based on an analogous principle. The vibration transmission through the interface between two solid objects is mainly controlled by the ratio of their mechanical impedances. Since the mechanical impedance is proportional to the material stiffness, the extremely soft element placed between two other objects works as an interface with high transmission loss of vibrations. Again, the majority of vibration energy is reflected or, in a system with concentrated parameters, dissipated on the internal damper of the source of vibration. The negligible amount of energy is transmitted or absorbed.

Early applications of these systems have been reported by Okubo [5] and Kodama [6]. The theoretical analysis of these systems was performed later by Mokrý [7, 8] and various applications of an active elasticity control technique in the noise and vibration control devices were demonstrated by Fukada [9, 10]. Finally, Imoto [11] and Takahara [12] demonstrated the great potential of this method on a system for suppressing vibrations by 20 dB in the broad frequency range from 1 to 100 kHz. On the other hand, results of these papers have indicated that the crucial issue limiting the efficiency of the system is the accurate adjustment of electrical circuit components of a negative capacitor. It results in the extreme sensitivity of the noise shielding or vibration isolation efficiency of the systems to changing operating conditions.

1.3   Summary of the main gaps in the state of the art addressed by this Thesis

Practical realization of PSAC systems suffers from a high sensitivity accompanied by a low stability and a deteriorating efficiency even in slightly varying operating conditions. Although a research in the recent years achieved partial accomplishments in laboratory conditions, mostly only fundamental principles have been verified. However, heretofore developed techniques do not offer a sufficient ground for the realization of a robust device. The substantial deficiency of devices based on PSAC with the negative capacitor can be marked as their inability to adapt on variable operating conditions.

1.4   Goals of the Thesis

The general goal of this Thesis is to work up a design of PSAC-based vibration isolation and noise shielding systems with a negative capacitor in order to achieve

their reliable operability in variable real world conditions. The work focuses on designing self-adaptive systems able to achieve and sustain high efficiency of a vibration isolation and a noise shielding.

1.5   Outline of the Thesis

The Thesis is organized in five parts:

Part I: Background An introduction and a literature review of the state of the art in the field of active noise and vibration control are presented.

Part II: Vibration isolation system This part presents principles of the vibration isolation by the PSAC method with the negative capacitor and the general stability conditions are calculated.

    Chapter 4: The design and optimization of the negative capacitor circuitry.

    Chapter 5: The design of a mechanism of the negative capacitor adaptation.

    Chapter 6: Experimental measurements of a vibration isolation efficiency.

Part III: Noise shielding system This part largely follows the analogy with Part II "Vibration isolation system". The same steps are completed in the same order and an adaptive noise shielding system is designed, analyzed, and experimentally verified.

Part IV: Analysis of flexural modes of a clamped membrane motion This part presents a detailed calculation of the response of a thin piezoelectric membrane to acoustic pressure.

Part V: Discussion and Conclusions The closing part summarizes the results achieved in the Thesis and points out the main achievements.

Appendices

    Appendix A: Description of an apparatus for a measurement of the vibration transmissibility.

    Appendix B: Transfer-function method and a description of a measurement apparatus for the measurement of the sound transmission loss.

    Appendix C: Verification of the results achieved in Part IV by measurement of a transmission loss of sound through the piezoelectric membrane.

    Appendix D: Verification of the results achieved in Part IV by measurements of a transmission loss of sound through a copper shell and its displacement in the acoustic field.

    Appendix E: List of my publications, preprints, and presentations.

VIBRATION ISOLATION BY THE PIEZOELECTRIC SHUNT ACOUSTIC CONTROL METHOD

2.1 Transmissibility of vibrations

Vibration of a system with concentrated parameters can be quantified by displacements $x_i(t)$, velocities $v_i(t) = \dot{x}_i(t)$, and accelerations $a_i(t) = \ddot{x}_i(t)$ as functions of time t in discrete locations i in the system. The vibration transmission between locations i and j is commonly characterized by a transmissibility $TR(j\omega)$ defined in the frequency domain:

$$TR(j\omega) = \left| \frac{A_j(j\omega)}{A_i(j\omega)} \right|.$$

Here $A_i(j\omega)$ and $A_j(j\omega)$ are frequency spectra of vibrations $a_i(t)$ and $a_j(t)$ measured at two locations i and j in the system.

2.2 Vibration isolation

Vibration isolation is understood by the prevention of vibration transmission between mechanically joined structures. When the stiffness $\mathcal{K}^*$ of the interface in the vibrating structure is reduced to zero, i.e. $\mathcal{K}^* \to 0$, transmissibility is necessarily reduced to zero as well $TR \to 0$. The important point is that it holds regardless the properties of the rest of the system. Therefore, the interface with the zero effective dynamic elastic stiffness ideally prevents the transmission of dynamic forces and, hence, isolates from vibrations. Such an element can be realized, at least in theory, by the piezoelectric actuator connected to the circuit that behaves as a negative capacitor.

2.3   Ideal vibration isolation system with an ideal negative capacitor

We consider a vibrating structure with the interface realized by a piezoelectric actuator connected to the external one-port circuit (negative capacitor) as illustrated in Fig. 2.1. If one considers the special case of the piezoelectric n-layer stack
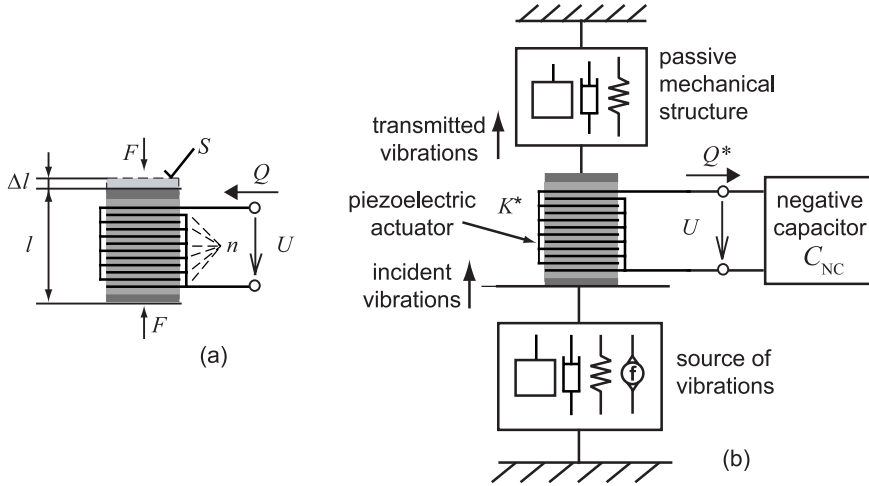
Figure 2.1: Vibration isolation system with the piezoelectric actuator: (a) the n-layer piezoelectric stack actuator, (b) the vibrating structure with the interface realized by the imbedded piezoelectric actuator, which is connected to the negative capacitor.

actuator of a cross-section area S, which is perpendicular to the actuator length l, and with a uniform uniaxial electrical and mechanical loading along the x_3 polar axis [see Fig. 2.1 (a)], the linear material state equations of the piezoelectric material can be simplified to the equations for the charge Q and the change of length Δl of the piezoelectric actuator in a following form:

$$Q \;=\; C_\mathrm{s}^F\, U + d\, F, \tag{2.1a}$$
$$\Delta l \;=\; d\, U + (1/k^U)\, F, \tag{2.1b}$$

 where C_s^F is the capacitance of a free piezoelectric actuator. Symbol U stands for the voltage on common electrodes of the actuator and the external circuit, symbols d and k^U are the piezoelectric and spring constants of the actuator, respectively.

Considering the requirement for the zero force transmitted through the piezoelectric actuator, $F = 0$, the condition which is to be satisfied by the ideal shunt circuit can be found as follows:

$$C_\mathrm{NC}^{(\mathrm{id})} = -C_\mathrm{s}^F, \tag{2.2}$$

where $C_{\mathrm{NC}}^{(\mathrm{id})} = Q^*/U$ is the ideal capacitance of the shunt circuit, which induces zero effective elastic stiffness of the piezoelectric element with capacitance C_{s}^{F}. At this moment, the main attention in a realization of the vibration isolation system should be drawn to the design of an active circuit - the negative capacitor - with parameters which satisfy the condition in Eq. (2.2).

2.4 Real vibration isolation system with a real negative capacitor

The realization of an ideally working system is fundamentally impossible and only less or more accurate approach of the real systems to a desired ideal state can be achieved. Therefore, capacitances C_{NC} and C_{s}^{F} are generally different and one can obtain from Eqs. (2.1) together with equation $C_{\mathrm{NC}}^{(\mathrm{id})} = Q^*/U$ a dependence of the effective elastic stiffness $\mathcal{K}^*$ on C_{NC} :

$$\frac{\mathcal{K}^*}{k^U} = \left(1 - \frac{\kappa^2}{1 + C_{\mathrm{NC}}/C_{\mathrm{s}}^{F}}\right)^{-1},\tag{2.3}$$

where $\kappa^2 = d^2 k^U/(l C_{\mathrm{s}}^{F})$ is the electromechanical coupling factor of the piezoelectric actuator. Absolute values of the fraction given by Eq. (2.3) are plotted in Fig. 2.2.
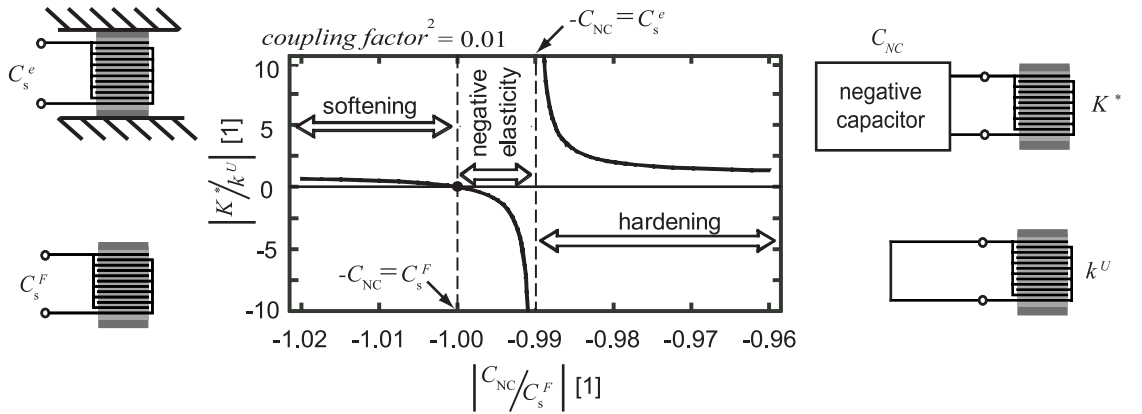
Figure 2.2: Dependence of the relative effective elastic stiffness of the piezoelectric sample on the ratio of the shunt capacitance to the capacitance of the sample. This characteristic was experimentally verified in [9].

At this moment, the transmissibility can be conveniently expressed in terms of capacitance difference $\Delta C = C_{\mathrm{NC}} + C_{\mathrm{s}}^{F}$ as follows:

$$TR = \left|1 + j\omega \mathcal{Z}_2\left(\frac{1}{k^U} - \frac{d^2}{\Delta C}\right)\right|^{-1},\tag{2.4}$$

where $\mathcal{Z}_2$ is the mechanical impedance of the passive mechanical structure placed on the piezoelectric actuator. Equation (2.4) determines the transmissibility in non-ideal state, when the capacitances of the circuit and the actuator differ, i.e. $|\Delta C| > 0$.

2.5   Vibration isolation with a piezoelectric actuator shunted with a negative capacitor: Formulation of the problem

The Thesis analyzes the crucial issues of the sensitivity and stability of real vibration isolation system on changes in operating conditions. On that base, demands for the optimally adjusted real vibration isolation system composed of a piezoelectric actuator and a shunt circuit are formulated as to **design and realize circuit that behaves as a negative capacitor and satisfies three conditions:**

Minimal $|\Delta C|$ for all frequencies, which set the system close to the ideal state on the edge of stability.

Positive real part of the impedance of the element which is created as a parallel combination of the negative capacitor and the actuator for all nonzero frequencies. This protects the system against oscillations.

Negative sign of static capacitances difference, i.e. $\Delta C(j\omega) < 0$ **for** $\omega = 0$**,** which secures a static stability of the system.

2.6   Vibration isolation system with the automatic adaptation of the negative capacitor

The fundamental concept of the automatic adjustment proposed in this work is shown in Fig. 2.3. The piezoelectric force sensor is placed under the piezoelectric actuator to measure the transmitted force F. The force sensor is connected to the charge amplifier with a small input impedance and produces the piezoelectric charge proportional to the transmitted force $Q_F = d_F\,F$, where d_F is an effective piezoelectric constant of the force sensor. The charge Q_F is converted to a voltage $U_F = a_F Q_F$ by the charge amplifier. Symbol a_F stands for the charge-voltage conversion constant. The voltage U on the common electrodes of the actuator and the negative capacitor is introduced to the high-input-impedance instrumentation amplifier, which produces a voltage $U_A = a_A U$. Constant a_A is the differential gain of the amplifier.
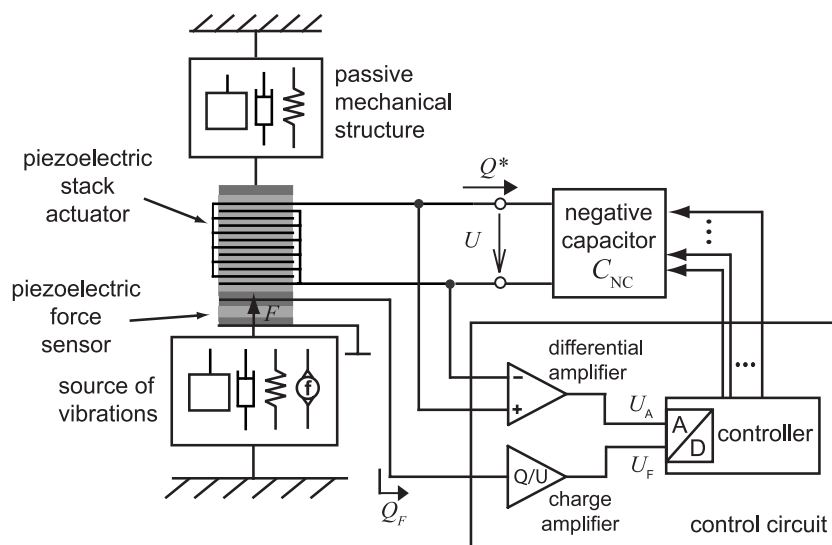
Figure 2.3: Basic diagram of automatic adaptation introduced to the vibration isolation system.

The task for the control circuit is to process the voltages U_F and U_A, on that base evaluate the vibration isolation efficiency of the system, and possibly correct an arbitrary number of parameters of the negative capacitor if the efficiency deteriorates. The described feedback allows the vibration isolation system to adapt itself on unwanted changes in the operating conditions.

The specific design of the self-adaptive system realized in the Thesis evolved in the final form with the block circuit diagram depicted in Fig. 2.4. Simplified version of the system depicted on Fig. 2.4 was suggested and realized in the diploma Thesis by Miloš Kodejška (see Fig. 2.5).

Evaluation of the vibration isolation efficiency

Transmissibility is the quantity that determines the efficiency of the vibration isolation. Since the effective elastic stiffness of the actuator controls the transmissibility of vibrations, we can profitably use the effective elastic stiffness as a relevant quantity for the estimation of the transmissibility of vibrations.

If the controlled system is in the proximity of the ideal state $\left(\frac{\mathcal{K}^*}{k^U} \ll 1\right)$, we can write the approximative relation $U_A \approx (a_A/d)\Delta l$ and estimate the effective elastic stiffness of the piezoelectric actuator from relation:

$$\mathcal{K}^* = \frac{F}{\Delta l} \approx \frac{a_A}{a_F d_F d} \frac{U_F}{U_A}. \tag{2.5}$$

Equation (2.5) gives the essential information for the feedback control of the vi-
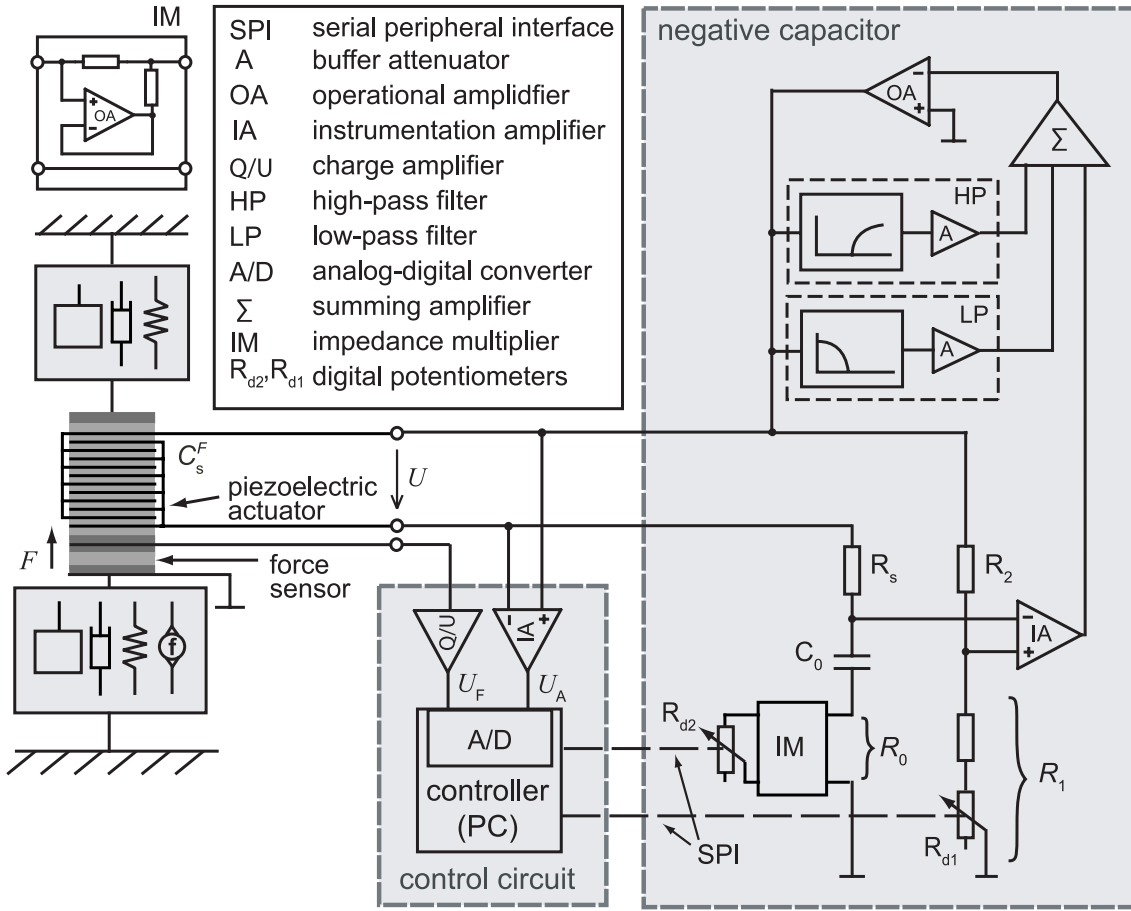
Figure 2.4:   Schema of the vibration isolation system with the negative capacitor and the control circuit.

bration isolation system. The ratio of the measured voltages U_F/U_A can be regarded as an error value. Therefore, we reformulate the task for the control circuit as the setting parameters of the negative capacitor to minimize the absolute value of the measured error value:

$$\min \left| \frac{U_F}{U_A} \right| \Rightarrow \text{optimal adjustment of the vibration isolation system.} \qquad (2.6)$$

In order to determine the control law, we find dependence of the reciprocal value of the error U_F/U_A on the negative capacitor parameters using Eqs. (2.3) and (2.5) as follows:

$$\frac{U_A}{U_F} \approx \frac{a_A}{a_F d_F d k^U} \left(1 + \kappa^2 \frac{C_s^F}{\Delta C} \right). \qquad (2.7)$$
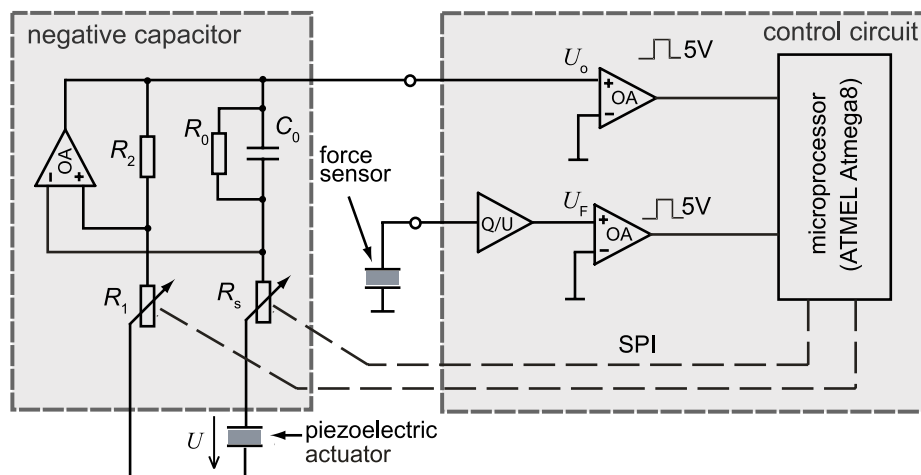
Figure 2.5: Electrical scheme of the negative capacitor with a control circuit in the self-adjusting vibration isolation system. Voltage U_F is a converted signal from the force sensor, which measures the transmitted force F. Voltage U applied to the piezoelectric actuator is proportional to the change of length Δl of the piezoelectric actuator. The transmissibility of vibrations controlled by the negative capacitor can be estimated from the phase difference of $U_\text{o}/U_F\,\Delta l$.

Equation (2.7) determines approximately the function $U_\text{A}/U_F = f(\Delta C)$. However, it is clear that its value is significantly sensitive to any variation of ΔC in the proximity of $\Delta C = 0$ and changes both with whatever unpredictable variation of system parameters and with the intentional control of circuit parameters. Consequently, the suitable control of chosen parameters can compensate the unwanted mistuning of the system caused by external effects and thereby it can minimize the vibration transmissibility.

Adaptation of the negative capacitor parameters

Two parameters, R_1 and R_0, of the circuit shown in Fig. 2.4 are chosen to be controlled. Their values complementarily control both resistive and capacitive parts of the negative capacitor capacitance. Hence from Eq. (2.7), we estimate the relation:

$$\frac{U_\text{A}}{U_F} \approx \frac{a_\text{A}}{a_F d_F dk^U}\left(1 + \kappa^2 \frac{C_\text{s}^F}{\Delta C(R_1,\,R_0)}\right). \tag{2.8}$$

Function (2.8) is proportionally plotted in graphs in Fig. 2.6 for the single frequency ω_m and in the close proximity of the optimal adjustment $[R_1^{(\text{o})},\,R_0^{(\text{o})}]$.
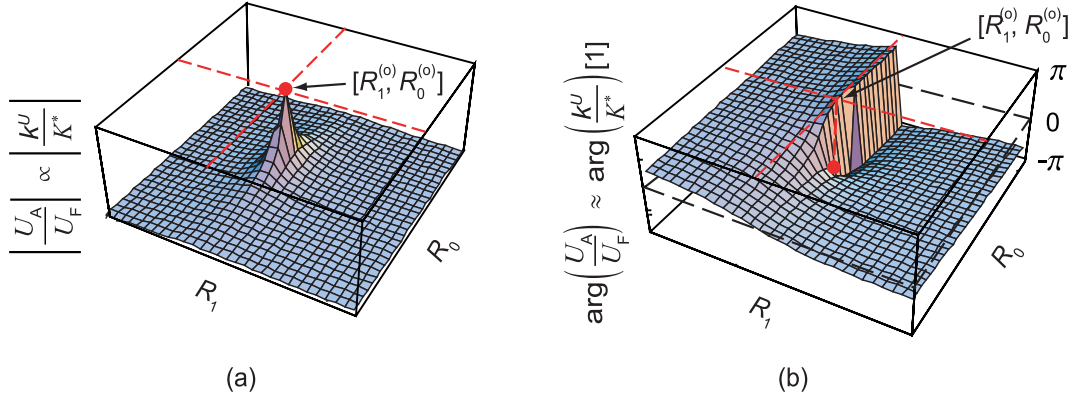
Figure 2.6: Proportional dependence of (a) amplitude and (b) phase of voltage ratio U_A/U_F and relative elastic stiffness $k^U/\mathcal{K}^*$ on resistances R_1 and R_0 at single frequency. The graph is plotted without any concrete values because these can not be evaluated without significant inaccuracy. The only relevant information is the proportion. The point of optimal adjustment $[R_0^{(o)}, R_1^{(o)}]$ is desired to be approached.

Control law

Value of U_A/U_F is the input information from which the control circuit determines whether and possibly how to change the values of resistors R_1 and R_0 in the negative capacitor. For that purpose, we define quadrants of the "R-plane" (plane of R_1 and R_0) as the areas separated by lines $R_1 = R_1^{(o)}$ and $R_0 = R_0^{(o)}$. These lines are emphasized in Fig. 2.6 as the red dashed ones. The point at their intersection $[R_1^{(o)}, R_0^{(o)}]$ stands for the optimal adjustment.

The optimal point can not be directly evaluated from the measured value of U_A/U_F since the function $U_A/U_F = f(R_1, R_0)$ is found only approximately for a simple model. Moreover, as follows from the sensitivity analysis, location of the optimal point is significantly sensitive and shifts with even small variations in the operating conditions. The only utilizable information is the relative proportion of the graph. For that reason, the control algorithm is proposed as iterative and we define the step of each iteration by values of ΔR_1 and ΔR_0 as follows:

$$R_{1,i+1} = R_{1,i} + \Delta R_1,$$
$$R_{0,i+1} = R_{0,i} + \Delta R_0.$$

Here $R_{1,i+1}, R_{1,i}$ and $R_{0,i+1}, R_{0,i}$ are the "new" and "old" values of resistors R_1 and R_0, respectively. Now the task for the control circuit is reduced to decide the steps ΔR_1 and ΔR_0 from the measured value of U_A/U_F.

The control law can be easily suggested if one plots the curves of the cuts through the plane $\arg(U_A/U_F) = f(R_1, R_0)$ as shown in Fig. 2.7. This graphs re-
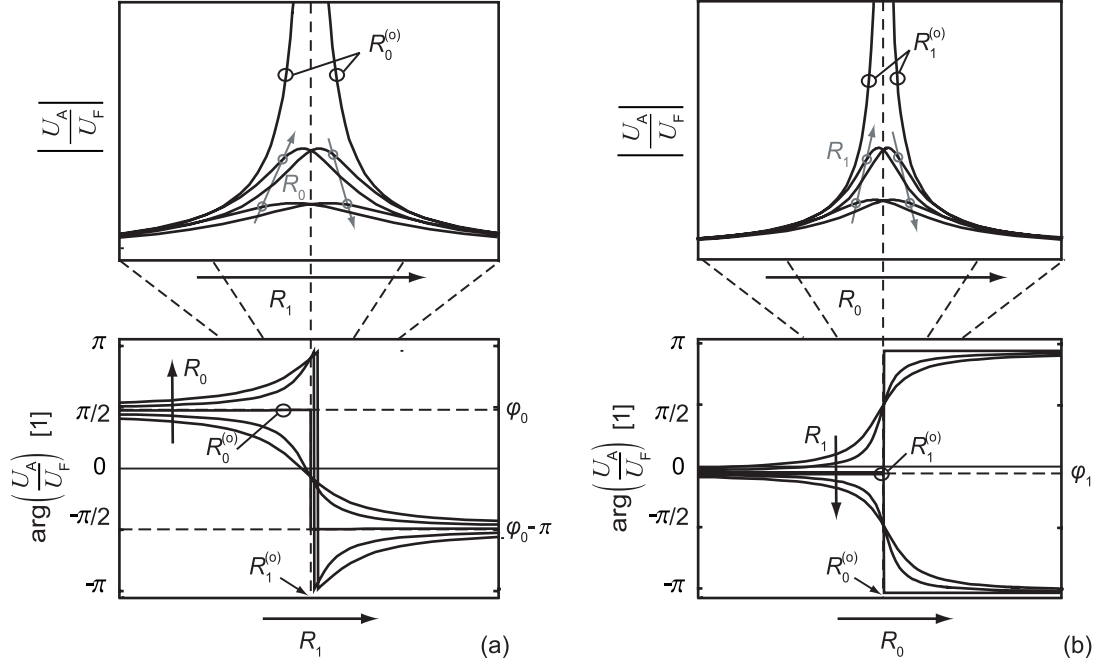
Figure 2.7: Proportional dependence of U_A/U_F on (a) resistances R_1 with constant R_0 and (b) resistances R_0 with constant R_1 at constant frequency.

veal that $\arg\left(U_A/U_F\right)$ can positively determine the quadrant of R-plane, in which the point $[R_1, R_0]$ actually lies. Therefore, determination of the sign and length of the control step is proposed as follows:

$$
\Delta R_1 =
\begin{cases}
+a_{R1}\left|\dfrac{U_F}{U_A}\right| & \text{for} \quad \arg\left(\dfrac{U_A}{U_F}\right) \in \left(\varphi_1 + 2k\pi, \varphi_1 + (2k+1)\pi\right\rangle \\[2mm]
-a_{R1}\left|\dfrac{U_F}{U_A}\right| & \text{for} \quad \arg\left(\dfrac{U_A}{U_F}\right) \notin \left(\varphi_1 + 2k\pi, \varphi_1 + (2k+1)\pi\right\rangle
\end{cases}
\tag{2.9a}
$$

$$
\Delta R_0 =
\begin{cases}
+a_{R0}\left|\dfrac{U_F}{U_A}\right| & \text{for} \quad \arg\left(\dfrac{U_A}{U_F}\right) \in \left(\varphi_0 + (2k-1)\pi, \varphi_0 + 2k\pi\right\rangle \\[2mm]
-a_{R0}\left|\dfrac{U_F}{U_A}\right| & \text{for} \quad \arg\left(\dfrac{U_A}{U_F}\right) \notin \left(\varphi_0 + (2k-1)\pi, \varphi_0 + 2k\pi\right\rangle.
\end{cases}
\tag{2.9b}
$$

Meaning of Eqs. (2.9) is graphically interpreted in Fig. 2.8. There as well as in Eqs. (2.9) and in Fig. 2.7 angles φ_1 and φ_0 are crucial parameters which can be accurately determined only by an experimental calibration. The factors $a_{R1}\left|U_F/U_A\right|$ and $a_{R0}\left|U_F/U_A\right|$ determine the length of the step. The parameters a_{R1} and a_{R0} together with the period of iteration control speed and the form of the adjustment convergence. Their values are best determinable again only by experimental calibration.
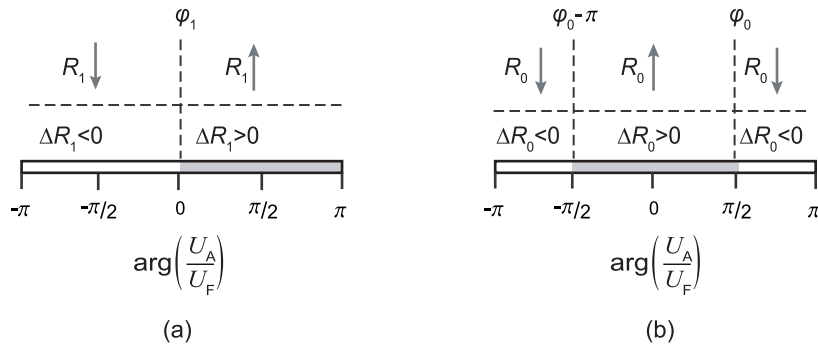
Figure 2.8: Interpretative illustration of the readjustment step evaluation.

2.7   Vibration isolation: Experiment

Measurement of the vibration isolation efficiency follows an evaluation of the vibration transmissibility defined as:

$$TR_{\mathrm{dB}}(j\omega) = 20 \log_{10} \frac{|A_{\mathrm{t}}(j\omega)|}{|A_{\mathrm{i}}(j\omega)|},$$

where $|A_{\mathrm{t}}(j\omega)|$ and $|A_{\mathrm{i}}(j\omega)|$ are amplitudes of acceleration of transmitted and incident vibrations, respectively.

The process of transmissibility measurement is performed in four layers: sensing, pre-amplification, data acquisition, and evaluation as illustrated on Fig. 2.9.
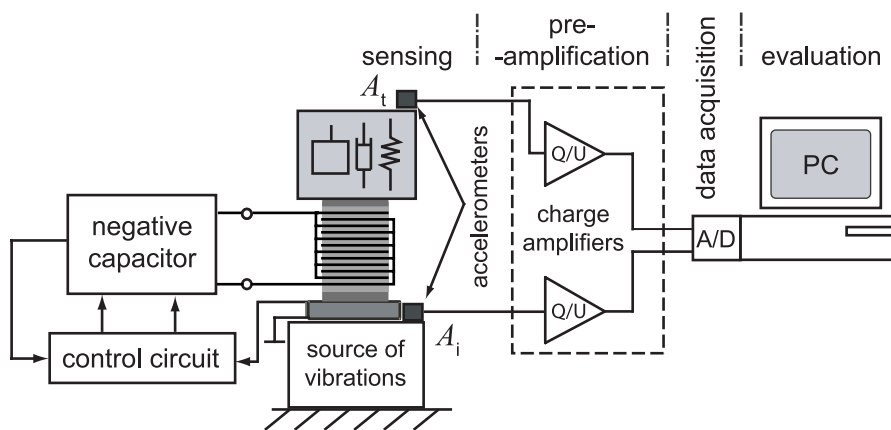
Figure 2.9: Vibration transmissibility measurement.

Vibration isolation system with a control circuit realized by a personal computer

Measurements presented in this section were carried out with the negative capacitor and the control circuit with the design shown in Fig. 2.4. The time dependence of the relative transmissibility level defined as $\Delta TR_{dB}(t) = TR_{dB}(t) - TR_{dB,off}$, where $TR_{dB,off}$ is the transmissibility when the negative capacitor is disconnected, is shown in Fig. 2.10. In this experiment, the negative capacitor was connected
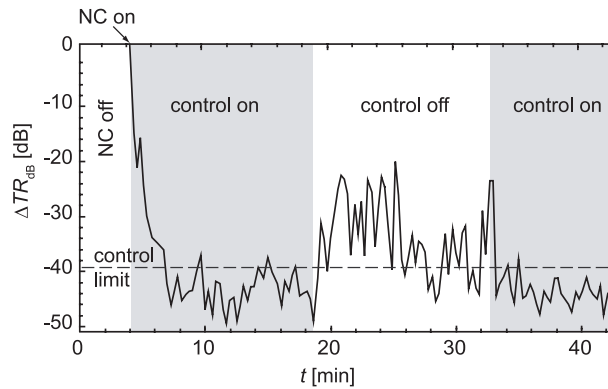
Figure 2.10: Time dependence of the relative transmissibility level $\Delta TR_{dB}(t)$ of harmonic vibrations at frequency $f = 1\,\mathrm{kHz}$. Gray areas indicate regions where the control circuit is turned on.

to the piezoelectric actuator at the time $t = 4\,\mathrm{min}$ in the graph. Simultaneously, the control circuit was turned on. The transmissibility level decreased under the control limit value $-40\,\mathrm{dB}$, i.e. the point where the iteration step was zero.

At the time $t = 18.3\,\mathrm{min}$, the control circuit was turned off and the relative transmissibility level increased quickly by $20\,\mathrm{dB}$. At the time $t = 32.3\,\mathrm{min}$, the control circuit was turned on again and the relative transmissibility level decreased under the value $-40\,\mathrm{dB}$.

Vibration isolation system with a control circuit realized by an integrated microprocessor

Figure 2.11 shows two time-dependencies of levels of the vibration transmissibility at frequency $f = 0.6\,\mathrm{kHz}$ through the vibration isolation system (see Fig. 2.5) exposed to heating in two situations. The black line corresponds to the situation, when the control circuit was turned off and the initial drop in the transmissibility of vibrations by $20\,\mathrm{dB}$ deteriorated by $10\,\mathrm{dB}$ within 5 minutes. The gray line corresponds to the situation when the control circuit was turned on. In this case,
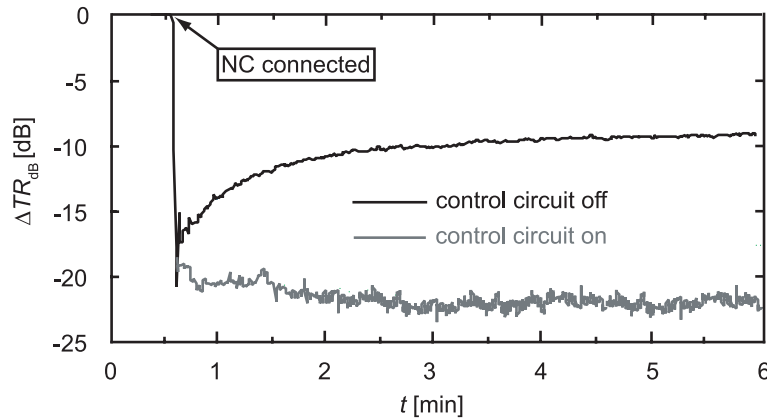
Figure 2.11:   Effect of changing operational conditions (heating) on the time dependencies of transmissibility of vibrations of frequency $f = 0.6\,\text{kHz}$ through the self-adjusting vibration isolation system in two situations, when the control circuit was turned off (black line) and turned on (gray line).

actions of the control circuit yielded the long-time sustainable value $20\,\text{dB}$ of transmissibility of vibrations.

Figure 2.12 shows the effect of the vibration excitation frequency on the transmissibility of vibrations in two situations. The solid line corresponds to the situation when the negative capacitor was adjusted at $1\,\text{kHz}$ and kept fixed during the experiment and the dashed line corresponds to the situation when the self-adjustment control circuit applied corrections to the negative capacitor adjustment.
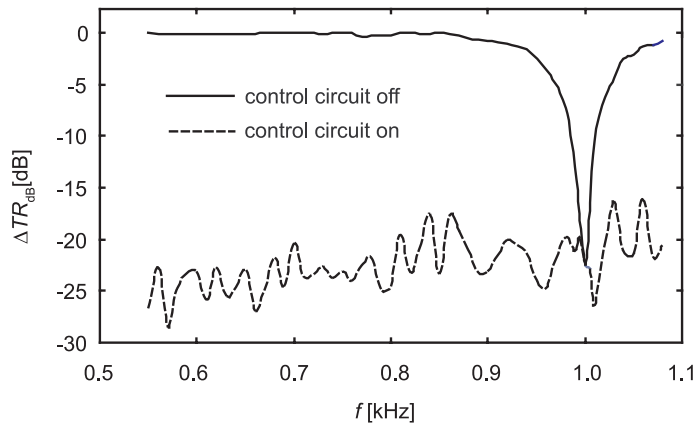
Figure 2.12: Effect of frequency change of a vibration excitation on the transmissibility of vibrations through the self-adjusting vibration isolation system: first, with the fixed adjustment of negative capacitor (solid line) and, second, with adjustment corrections applied by the control circuit (dashed line).

NOISE SHIELDING BY THE PIEZOELECTRIC SHUNT ACOUSTIC CONTROL METHOD

This chapter introduces a method of the sound control based on the active interface which is designed in order to achieve desired impact on the sound transmission, in particular case, the noise shielding. The basic concept for the analysis, design, realization, and measurement of the noise shielding system with the piezoelectric curved membrane made of polyvinylidene fluoride (PVDF) is shown in Fig. 3.1.
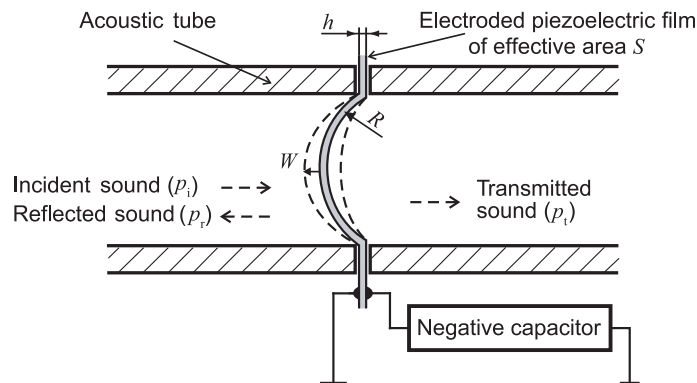
Figure 3.1: The fundamental concept of noise shielding barrier used for analysis, design, and measurement in this Thesis.

3.1 Acoustic transmission loss of sound: noise shielding

The function called the acoustic transmission loss TL, which is defined as

$$TL = -20 \log_{10} \left| \frac{p_\text{t}}{p_\text{i}} \right|, \tag{3.1}$$

is often measured to evaluate the noise shielding efficiency. Here p_i and p_t are acoustic pressures of the incident and transmitted sound waves, respectively. Meakawa [13] published a formula for the acoustic transmission loss of sound TL through the barrier in terms of its acoustic impedance z_m as follows:

$$TL = 20 \log_{10} \left| 1 + \frac{z_m}{2\rho_0 c} \right|. \tag{3.2}$$

Here c is the sound velocity in air and ρ_0 is the volume mass density of air. Further, Mokrý [7] calculated a simple formula for the acoustic impedance of the curved membrane, which has a uniform radial displacement along the whole membrane surface:

$$z_m = jh \left(\omega\rho - \frac{Y^*(j\omega)}{\omega R^2} \right), \tag{3.3}$$

where the symbol $Y^*(j\omega)$ denotes the complex Young's modulus, ρ is the mass volume density of the membrane, R is the radius of the membrane curvature, and h stands for the membrane thickness as indicated in Fig. 3.1. One can see from Eqs. (3.3) and (3.2) how the transmission loss is controlled by the membrane geometry, mass, and stiffness.

The desired ideal sound barrier should ideally achieve infinity transmission loss of sound through the membrane. This can be obviously achieved using a membrane with the infinity elastic stiffness. Then the condition for an ideal noise reflection and hence noise shielding is simply defined as follows:

$$Y^*(j\omega) \to \infty. \tag{3.4}$$

3.2   Ideal noise shielding system with the ideal negative capacitor H

Calculation analogical to the one performed in Section 2.3 reveals the condition for the ideal shunt negative capacitor properties in the ideal noise shielding system, which is:

$$C_{NC}^{(id)} = -C_s^e. \tag{3.5}$$

Here $C_{NC}^{(id)}$ is the capacitance of the ideal shunt negative capacitor and C_s^e is the capacitance of the clamped piezoelectric membrane.

3.3 Real noise shielding system with a real negative capacitor for hardening mode

Problematic issues concerning real noise shielding systems based on the PSAC method are analogical to the ones introduced in the case of the vibration isolation (see Section 2.4). The studied PSAC systems suffer from difficulties in their sustainable adjustment which should ideally approach and hold the condition Eq. (3.5) in a broad frequency band and from the fact that the ideally working system is in principle at the edge of stability.

In a real system, capacitances $-C_{\mathrm{NC}}$ and C_{s}^{e} are generally different and one can obtain the dependence of the effective Young's modulus Y^{*} on the capacitance C_{NC} as follows:

$$\frac{Y^{*}}{Y_{0}^{U}} = \left(1 + \frac{\kappa^{2}}{1 + C_{\mathrm{NC}}/C_{\mathrm{s}}^{e}}\right). \tag{3.6}$$

Here κ^{2} is the electromechanical coupling factor of the piezoelectric membrane. Equation (3.6) describes identical effect as Eq. (2.3) for the case of an actuator in the vibration isolation system. Therefore the dependence of the fraction of Young's modulus Y^{*}/Y_{0}^{U} vs. the fraction of capacitances $C_{\mathrm{NC}}/C_{\mathrm{s}}^{e}$ is included in Fig. 2.2 as well, if we assume proportional relation of Young's modulus and elastic stiffness, i.e. $k^{U} \sim Y_{0}^{U}$ and $\mathcal{K}^{*} \sim Y^{*}$. .

Another problematic issue, which is unavoidable in the noise shielding system, emerges from the shape of the shielding element. A thin curved membrane necessarily exhibits flexural motion with complicated dynamics. The detailed extensive study of the membrane dynamics, is presented in separate Part IV of the Thesis. The only resulting formula for the transmission loss is introduced herein in the terms of acoustic impedances and capacitance difference $\Delta C_{e} = C_{\mathrm{s}}^{e} + C_{\mathrm{NC}}$ as follows:

$$TL = 20 \log_{10} \left| 1 + \frac{z_{\mathrm{m}}}{2z_{\mathrm{a}}} + \kappa^{2} \frac{z_{\mathrm{m}}^{(\mathrm{e})}}{2z_{\mathrm{a}}} \frac{C_{\mathrm{s}}^{e}}{\Delta C_{e}} \right|. \tag{3.7}$$

In this formula

$$z_{\mathrm{a}} = c\rho_{o} \quad \text{and} \quad z_{\mathrm{m}} = \frac{1}{\mathfrak{S}} \left(z_{\mathrm{m}}^{(\mathrm{m})} + z_{\mathrm{m}}^{(\mathrm{e})} \right)$$

are the acoustic impedances of air and the membrane, respectively. The symbol $\mathfrak{S}$, is a dimensionless coefficient expressed and comprehensively analyzed in Chapter 11 of the Thesis. Here, it is worth mentioning that this dimensionless coefficient introduces the modal membrane manifestation into the resulting mechanical impedance z_{m}. In the approximation of the uniform membrane motion, the coefficient $\mathfrak{S}$ reaches 1.

Mechanical impedance of the membrane equals to the sum of two parts where $z_\mathrm{m}^{(\mathrm{m})} = j\omega h\rho$ is the contribution to mechanical impedance of the membrane controlled by its mass and $z_\mathrm{m}^{(\mathrm{e})} = -jhc_{11}^E/(R^2\omega)$ is the contribution to mechanical impedance of the membrane controlled by its elastic stiffness. The symbol c_{11}^E is the elastic stiffness proportional to the Young's modulus.

The aforementioned formula for the acoustic transmission loss was verified by a comparison with experimental data published by Fukada [10]. This verification is presented in Appendix C of the Thesis. Furthermore, the shape of a membrane displacement was analytically calculated from the theoretical analysis and a result was verified by an experimental measurement of a displacement of the curved copper membrane in a sound field. The copper membrane was used as relatively hard material with a small mechanical loss factor which markedly exhibits a flexural motion. This verification is presented in Appendix D of the Thesis.

3.4 Noise shielding with a piezoelectric curved membrane shunted with the negative capacitor: Formulation of the problem

The basic analysis performed above and the stability and sensitivity analysis presented comprehensively in the Thesis result in the following three crucial conditions imposed on the shunt negative capacitor which are to be addressed during the design of the noise shielding system. When we introduce $\Delta C_e = C_\mathrm{NC} + C_\mathrm{s}^e$ the real system needs to satisfy:

Minimal $|\Delta C_e|$ for all frequencies, which set the system close to the ideal state on the edge of stability.

Positive real part of the impedance of the element which is created as a parallel combination of the negative capacitor and the membrane for all nonzero frequencies. This protects the system against oscillations.

Positive sign of static capacitances difference, i.e. $\Delta C_e(j\omega) > 0$ for $\omega = 0$, which secures a static stability of the system.

3.5 Noise shielding system with the automatic adaptation of the negative capacitor

Mechanism of the automatic adjustment of the negative capacitor in the noise shielding system is analogical with the mechanism developed for the vibration

isolation system studied in Section 2.6. The arrangement of the noise barrier with two PVDF membranes and a "self-adaptive" negative capacitor is schematically shown in Fig. 3.2. The concept of a system adaptivity is based on sensing an error
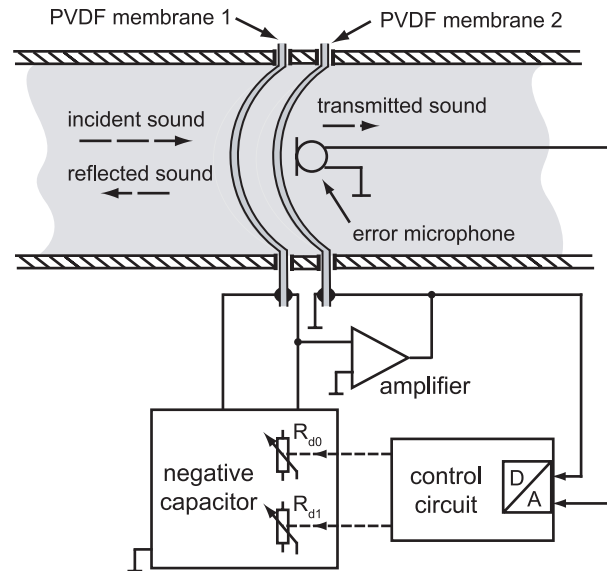
Figure 3.2: Block diagram of self-adaptive noise shielding system.

quantity - transmitted sound level - and a possible readjustment of two resistors of the negative capacitor in order to minimize the transmitted sound. The detailed arrangement of the negative capacitor with the additional amplifier and the personal computer, which represents a control circuit, is shown in Fig. 3.3. The main part of the negative capacitor is a passive capacitor made of PVDF. This capacitor is prepared by the same technique and with the same dimensions as each of the membranes placed in the duct. Finally, this capacitor is reinforced by silicone, which prevents the motion of the PVDF capacitor. The reinforcement is introduced to keep the dielectric properties of the PVDF capacitor close to properties of the clamped sample as it is required for the proper characteristic of the negative capacitor.

Control algorithm

The control algorithm for the noise shielding system is almost identical with the algorithm for the vibration isolation system described in Section 2.6. The difference between them lies only in experimentally determined constants and their signs.

The main principle of the control algorithm can be described as follows. The acoustic transmission loss of sound through the curved piezoelectric membrane
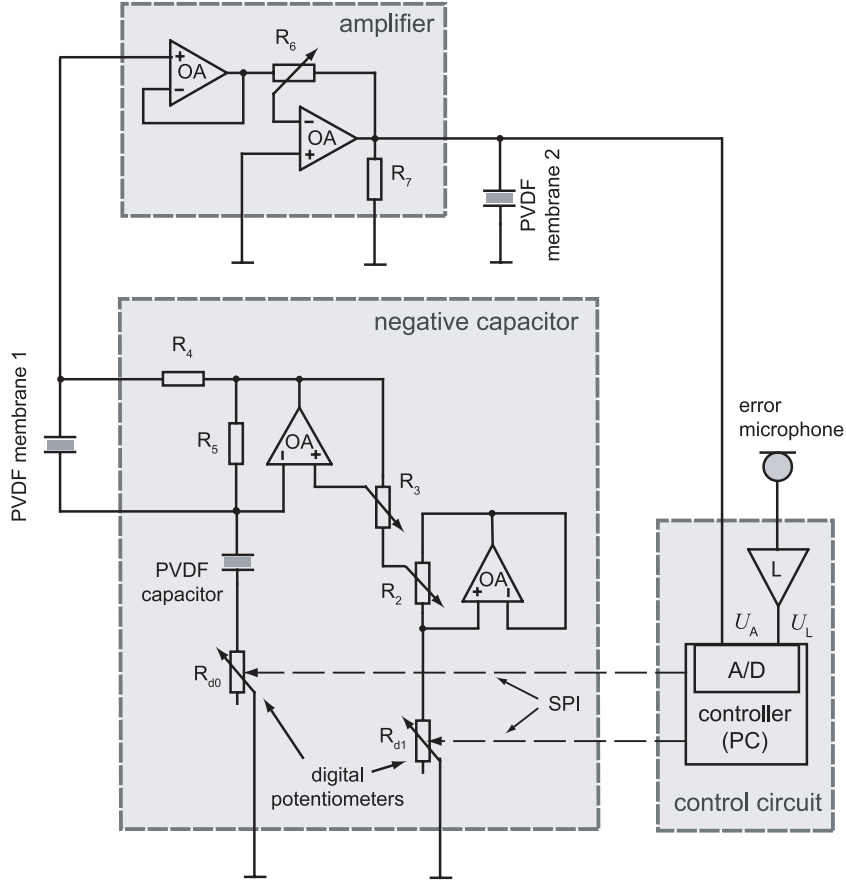
Figure 3.3: Electrical scheme of the self-adaptive noise shielding system.

can be estimated from voltages U_L and U_A . Firstly, the measured voltage U_L proportionally corresponds to the transmitted acoustic pressure p_t. Since the value of p_t is proportional to the amplitude of the membrane vibration in the radial direction, it is also proportional to the in-plane membrane elongation Δl. Hence, the voltage U_L provides information on the in-plane elongation of the piezoelectric membrane, i.e. $\Delta l \propto U_\mathrm{L}$. In the situation, when the voltage-induced strain nearly cancels the force induced strain, the membrane elongation approaches zero and we can approximately write $dU \approx (1/Y_0^U)F$. Therefore, as the sensed voltage U_A is proportional to voltage U on a PVDF membrane 1, it provides information on the in-plane mechanical force applied to the piezoelectric membrane, i.e. $F \propto Y_0 U_\mathrm{A}$. Now it is convenient to denote the contribution to the acoustic transmission loss of the noise shielding system, which is controlled by the action of the piezoelectric membrane and the negative capacitor:

$$\Delta TL_\mathrm{NC} = TL(Y^*) - TL(Y_0) = 20 \log_{10}(Y^*/Y_0). \qquad (3.8)$$

When one considers that the effective Young's modulus of the membrane is given by the ratio of the in-plane force applied to the membrane over the total in-plane elongation of the membrane, i.e. $Y^* = F/\Delta l$, it is immediately obvious that the acoustic transmission loss controlled by the negative capacitor can be estimated from the signals introduced into the control circuit, i.e. $\Delta TL_{\mathrm{NC}} \propto 20 \log_{10}(U_{\mathrm{A}}/U_{\mathrm{L}})$. In order to keep considerably high values of function ΔTL_{NC}, the control circuit processes the amplitude of the ratio $U_{\mathrm{A}}/U_{\mathrm{L}}$ and the phase difference between signals U_{A} and U_{L} and applies corrections to the digital potentiometers R_{d0} and R_{d1} in the negative capacitor.

The rules for the estimation of resistor corrections are determined experimentally using a manual adjustment of the negative capacitor. If the phase difference between signals U_{L} and U_{A} belongs to the experimentally determined range (see illustration on Fig. 2.8), values of R_{d0} and R_{d1} are increased or decreased in order to maximize the ratio $U_{\mathrm{A}}/U_{\mathrm{L}}$ and, consequently, the estimated value of acoustic transmission loss ΔTL_{NC}.

3.6 Noise shielding: Experiment

This section presents results of measurement and experimental verification of functionality of the self-adaptive noise shielding system. The measurement of the acoustic transmission loss is carried out by a four-microphone transfer-function method modified for the use with two microphones (see Fig. 3.4).

Results of the measurement of the transmission loss through the noise shielding system

The frequency characteristics of transmission loss through the noise shielding barrier with circuitry shown in Fig. 3.3 were measured under two adjustments:

1. The negative capacitor was adjusted to suppress the sound transmission in a broad frequency band. The results of the measurement of the system which was set to suppress sound transmission maximally at the frequency $f = 3 \, \mathrm{kHz}$ is shown in Fig. 3.5.

2. The negative capacitor was adjusted to suppress the sound transmission in a narrow frequency band. The results of the measurement of the system with maximal sound transmission loss over 40 dB at frequency $f = 2 \, \mathrm{kHz}$ is shown on Fig. 3.6.
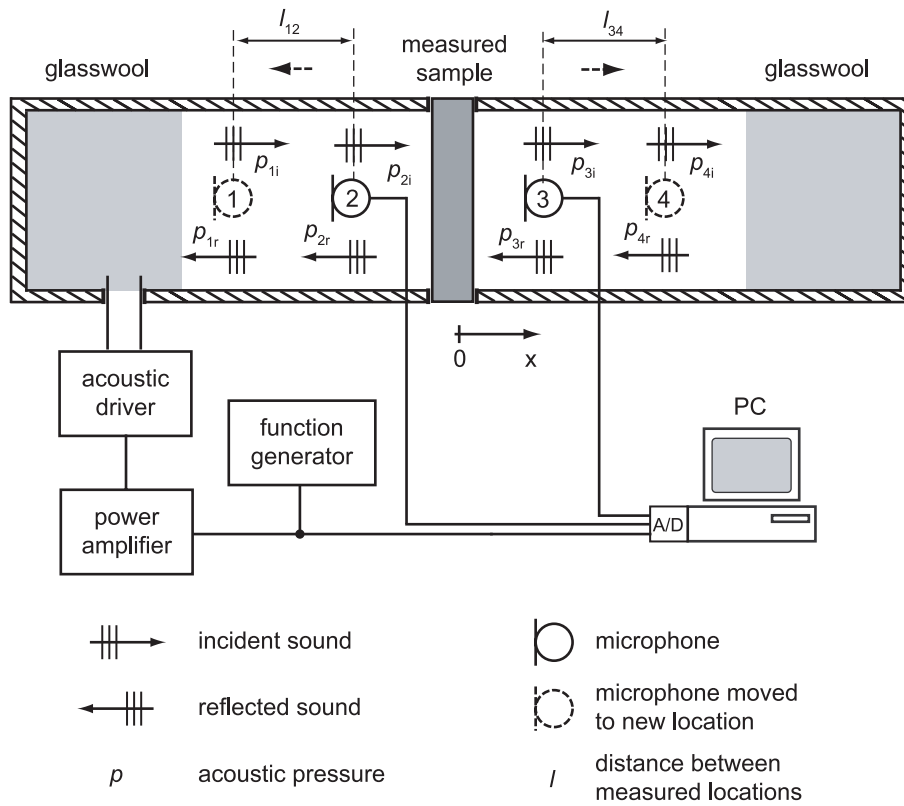
Figure 3.4: The Four-microphone method of a transfer-function measurement for a transmission loss evaluation. The method is adopted for two moving microphones. An acoustic pressures p are measured at least in four locations.

Measurement of a noise shielding efficiency in time

For purposes of the system adaptivity verification, the adjustment which results in the sound shielding in a narrow frequency band around frequency 1.6 kHz has been chosen. The measurement of an evolution of a noise shielding efficiency in time has been carried out with the measurement apparatus arranged as shown in Fig. 3.7. For the purposes of a transmission loss evaluation from the transmitted sound level measurement, the transmission loss difference is defined as

$$\Delta TL_{\mathrm{NC}} = L_{\mathrm{pt}}^{\mathrm{on}} - L_{\mathrm{pt}}^{\mathrm{off}}, \tag{3.9}$$

where $L_{\mathrm{pt}}^{\mathrm{on}}$ and $L_{\mathrm{pt}}^{\mathrm{off}}$ are sound levels measured when the negative capacitor is connected and disconnected, respectively.

Figure 3.8 shows measurements of the acoustic transmission loss through the adaptive noise shielding system. The measurement evaluates transmission loss of a single harmonic component of the sound of frequency f=1.6 kHz. The black
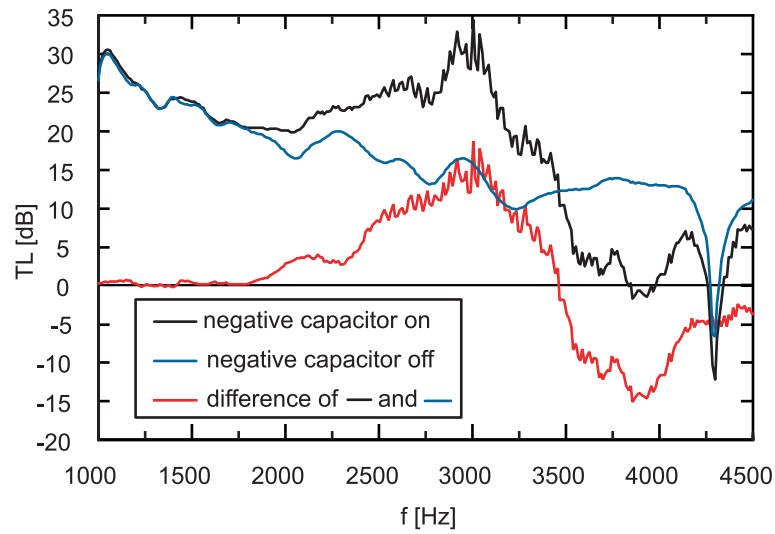
Figure 3.5: Broadband transmission loss achieved by the noise shielding system. The blue curve stands for the sound transmission loss through the membrane when the negative capacitor was disconnected. The black curve represents sound transmission loss when the negative capacitor was connected and adjusted and the red line stands for their difference.
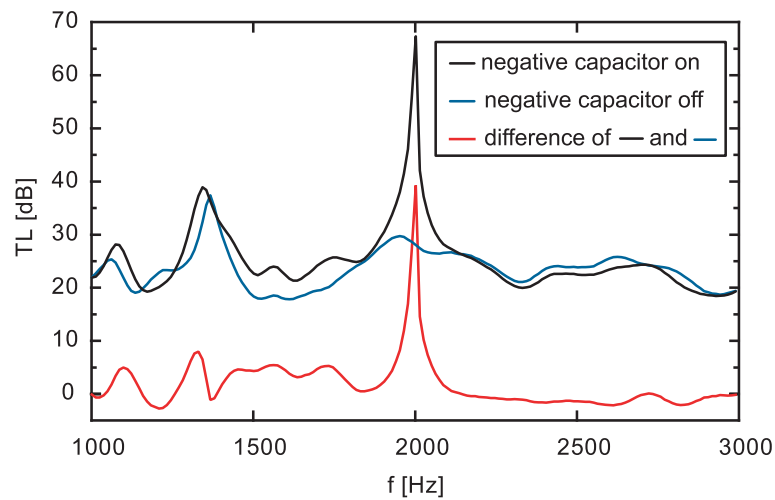
Figure 3.6: High transmission loss achieved by the noise shielding system on a narrow frequency band. The blue curve stands for the sound transmission loss through the membrane when the negative capacitor was disconnected. The black line represents sound transmission loss when the negative capacitor was connected and adjusted and the red line stands for their difference.

parts of the curve indicate the sound level measured when the control circuit was
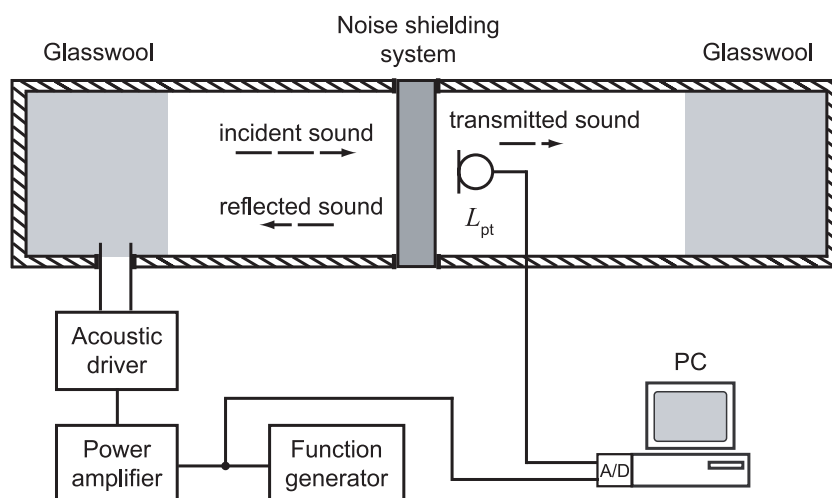
Figure 3.7: Measurement setup for measurement of time stability of the noise shielding system.
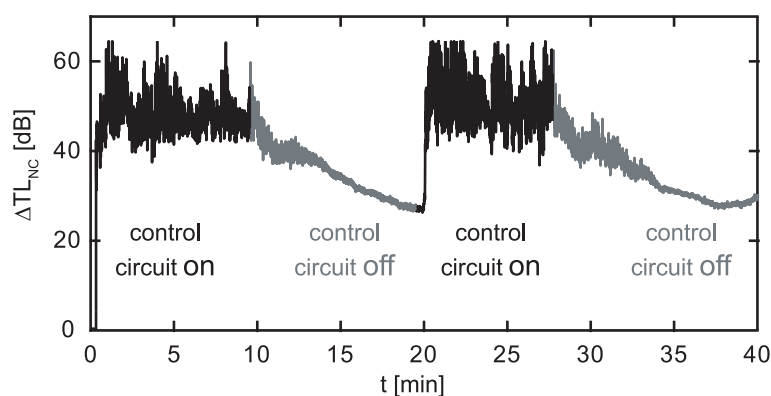
Figure 3.8: Measurement of the acoustic transmission loss through the adaptive noise shielding system. The black parts of the curve indicate the acoustic pressure level measured, when the control circuit was turned on. The gray parts of the curve indicate the acoustic pressure level measured, when the control circuit was turned off.

turned on and adjusts the system to maximally suppress the frequency f=1.6 kHz. The gray parts of the curve indicate the sound level measured, when the control circuit was turned off. The measurements have shown that when the negative capacitor was connected to the piezoelectric membrane and manually adjusted, an increase in the acoustic transmission loss by an additional 45 dB has been achieved resulting in the total acoustic transmission loss of about 65 dB. When the control circuit was turned on, we have demonstrated the long-term sustainable increase of the acoustic transmission loss by about 45 dB.

CONCLUSIONS

The method of piezoelectric shunt acoustic control with the negative capacitor was studied and worked up in the presented Thesis. It was shown that electric circuits which behave as negative capacitors can substantially affect an elastic response of the piezoelectric elements to which they are connected. Such piezoelectric elements imbedded into mechanical and acoustic systems were utilized as the principal components for a vibration isolation and a noise shielding.

Although the fundamentals of the studied methods have been well-developed and published in the past, the main achievement of the presented work lies in the analysis, design, and realization of the self-adaptive mechanism and its implementation to the real vibration isolation and the noise shielding systems. It was experimentally verified that the proposed ideas secure the sustainable high efficiency of the vibration isolation and the noise shielding, contrary to the situation, when no adaptation is employed. Although the developed adaptation mechanism was successfully verified only on a single harmonic component of the transmitted vibration and sound, the principle is essentially extensible to a broader frequency range.

The advantage of the developed approach to the construction of vibration isolation and sound shielding systems lies in the combination of a fast and simple analog negative capacitor, which can realize the active elasticity control of piezoelectric elements up to ultrasound frequencies [11, 12], with a digital control circuit, which just secures the proper adjustment of the electronic components in the negative capacitor. In this arrangement, there are almost no requirements on the minimum speed of the digital control circuit resulting in extreme simplicity and low cost of the electronic part of noise and vibration control systems. However, the control can also be theoretically performed by an analog circuit.

When this method is further extended to control the vibration transmissibility of the sound transmission in the broad frequency range, it will represent an alternative technique with potentials to supersede contemporary noise and vibration control systems in their numerous applications.

Bibliography

[1] R. L. Forward, "Electronic damping of vibrations in optical structures," *Applied Optics*, vol. 18, pp. 690–697, Mar. 1979.

[2] R. L. Forward and C. J. Swigert, "Electronic Damping of Orthogonal Bending Modes in a Cylindrical Mast-Experiment," *Journal of Spacecraft and Rockets*, vol. 18, pp. 5–10, Jan. 1981.

[3] D. Niederberger, *Smart Damping Materials using Shunt Control*. PhD thesis, Swiss Federal Institute of Technology, Zurich, Aug. 2005.

[4] M. Date, M. Kutani, and S. Sakai, "Electrically controlled elasticity utilizing piezoelectric coupling," *Journal of Applied Physics*, January 2000.

[5] T. Okubo, H. Kodama, K. Kimura, K.Yamamoto, E. Fukada, and M. Date, "Sound-isolation and vibration-isolating efficiency piezoelectric materials connected to negative capacitance circuits," in *Proc. 17th International Congress on Acoustics*, pp. 301–306, 2001.

[6] H. Kodama, T. Okubo, M. Date, and E. Fukada, "Sound reflection and absorption by piezoelectric polymer films," in *Proc. Material Research Society Symposium*, vol. 43, p. 698, 2002.

[7] P. Mokrý, E. Fukada, and K. Yamamoto, "Noise shielding system utilizing thin piezoelectric membrane and elasticity control," *Journal of Applied Physics*, 2003.

[8] P. Mokrý, E. Fukada, and K. Yamamoto, "Sound absorbing system as an application of the active elasticity control technique," *Journal of Applied Physics*, 2003.

[9] E. Fukada, M. Date, and H. Kodama *Materials Technology*, 2004.

[10] E. Fukada, M. Date, K. Kimura, T. Okubo, H. Kodama, P. Mokrý, and K. Yamamoto, "Sound isolation by piezoelectric polymer films connected to negative capacitance circuits," *IEEE Transactions on Dielectrics and Electrical Insulation*, 2004.

[11] K. Imoto, M. Nishiura, K. Yamamoto, M. Date, E. Fukada, and Y. Tajitsu, "Elasticity control of piezoelectric lead zirconate titanate (pzt) materials using negative-capacitance circuits," *Japanese Journal of Applied Physics*, 2005.

[12] K. Tahara, H. Ueda, J. Takarada, K. Imoto, K. Yamamoto, M. Date, E. Fukada, and Y. Tajitsu, "Basic study of application for elasticity control of piezoelectric lead zirconate titanate materials using negative-capacitance circuits to sound shielding technology," *Japanese Journal of Applied Physics*, 2006.

[13] Z. Maekawa and P. Lord, *Environmental and Architectural Acoustics*. Elsevier Science Ltd, 1994.

Publications, preprints, and presentations

- T. Sluka, H. Kodama, E. Fukada, and P. Mokrý, "Sound shielding by a piezoelectric membrane and a negative capacitor with feedback control," IEEE Transactions on Ultrasonics, Ferroelectrics, and Frequency Control. (accepted 1/2008)

  Presented at the conference PIEZO 2007, Liberec, Czech Republic, 2/2007. (poster)

- P. Mokrý, M. Kodejška, and T. Sluka, "On the vibration control using a piezoelectric actuator and a negative capacitor adjusted by a microprocessor." , in Proc. 16th IEEE International Symposium on Application of Ferroelectrics, 786-789, 27-31 May 2007.

  Presented at the 16th International Symposium on the Application of Ferroelectrics, Nara, Japan, 5/2007. (poster)

- T. Sluka and P. Mokrý, "Feedback control of piezoelectric actuator elastic properties in a vibration isolation system," Ferroelectrics, vol. 351, no. 1, pp. 51–61, 2007.

  Presented at the 8th European Conference on Applications of Polar Dielectrics, Metz, France, 9/2006. (oral presentation)

- Z. Plíva, M. Kolář, P. Došek, and T. Sluka, "Piezoelectric elements and their electronic driving with help of FPGA circuits," Ferroelectrics, vol. 351, no. 1, pp. 187-195, 2007.

  Presented at the 8th European Conference on Applications of Polar Dielectrics, Metz, France, 9/2006. (poster)

- T. Sluka and A. Kopal, "Extrinsic contributions to macroscopic properties of ferroic layer composites," Ferroelectics, vol. 319, pp. 171-180, 2005.

  Presented at 7th European Conference on Applications of Polar Dielectrics, Liberec, Czech Republic, 9/2004. (poster)

Unpublished talks

- "Noise and Vibration Control: Piezoelectric Shunting with a Negative Capacitor," Automatic Control Laboratory, ETH, Zurich, Switzerland, 08/2007.

- "Active sound isolation: automatic adjustment of the negative capacitance circuit," Kobayasi Institute of Physical Research, Tokyo, Japan, 12/2006.

- "Active vibration isolation: automatic adjustment of the negative capacitance circuit," Laboratory of Smart Structures and Materials, Kansai University, Osaka , Japan, 12/2006.

- "Extrinsic contributions to macroscopic properties of ferroic layer composites," The 1th International Symposium of Ph.D. students of the Euroregion Neisse, AE WGRiT, Jelenia Gora, Poland, 11/2004. (abstract treatise, ISBN 80-7083-966-X, XI, 2005)